Engineering and Technology Journal
Journal homepage: https://etj.uotechnology.edu.iq

Tire contact pressure effects on stress responses of scaled models of geotextile-reinforced flexible pavements over weak subgrade

Nawal D. Salman*, Hasan H. Joni

Department of Highways and Geotechnical Engineering, College of Civil Engineering, University of Technology-Iraq, Alsina'a street, 10066 Baghdad, Iraq.
*Corresponding author Email: bce.22.65@grad.uotechnology.edu.iq

HIGHLIGHTS

- The effect of tire contact pressure on geotextile-reinforced flexible pavements over weak subgrades were investigate.
- Increasing tire pressure raised the vertical stresses at the bottom at the asphalt layer and at the top of the subgrade.
- The use of geotextile reinforcement reduced stress transmission through the pavement layers.
- Reinforcement placed at mid-depth within the asphalt layer provided slightly better stress reduction.
- Overinflation can largely negate its structural benefits.

Keywords:
Tire Contact Pressure
Flexible Pavement
Geotextile
Pavement Reinforcement
Pavement Stress

ABSTRACT

Flexible pavements constructed over weak subgrades are subjected to premature failure due to excessive stress and deformation. Actual Tire contact pressure significantly affects the performance of flexible pavement. Geosynthetic reinforcement is used to overcome these issues. In this study, physical models with a (1/3) scale were used to investigate the effect of tire contact pressure on geotextile-reinforced flexible pavements over weak subgrades. Three pavement sections were studied: Control (unreinforced), Base-Surface reinforced with a non-woven geotextile, reinforced at the middle depth of the asphalt layer. Repeated axle loads were applied at three contact tire pressures of 480, 560, and 690 kPa, with vertical stresses measured at the bottom of the asphalt layer and at the top of the subgrade. Increasing tire pressure from 480 to 690 kPa raised vertical stresses at the asphalt bottom from 70.9% for the control section to 71.4 and 74.4% for sections 2 and 3, respectively. At the top of the subgrade, the same increase resulted in vertical stress rises from 58.9% for the control section to 73.7% and 83.6% for sections 2 and 3, respectively. Geotextile reinforcement effectively reduced subgrade stress at lower pressures, with middle depth reinforcement showing slightly better performance than surface–base interface reinforcement. However, the reinforcement benefits diminished under high contact tire pressures. The results revealed that tire pressure constitutes a fundamental factor that affects pavement performance, especially when built over weak subgrades, while optimized geotextile placement further contributes to performance gains.

1. Introduction

Flexible pavements are widely used in highway construction due to their lower initial costs, ease of construction, and relatively simple maintenance requirements. These pavements typically consist of multiple layers, including the asphalt surface (wearing course), a base, a subbase, and a subgrade. The primary function of this layered system is to distribute traffic loads from the surface down to the subgrade. However, the performance of flexible pavements is highly dependent on subgrade strength and the system's ability to spread stresses effectively. When built over weak subgrades, these pavements are prone to early failures such as rutting, cracking, and excessive settlement [1]. To address these challenges, geosynthetic materials such as geotextiles and geogrids are commonly incorporated into pavement structures [2-4]. These reinforcements enhance load distribution, minimize deformation, and extend pavement service life. Geosynthetics can be installed at various interfaces—between the base and subgrade, between the base and subbase, or even within the granular base layer—to improve the structural integrity of the system [3-7]. Reinforced pavements have been shown to impose lower stresses on the subgrade, thereby reducing the risk of failure [8].

The reinforcement mechanism of geosynthetics operates through several functions: lateral restraint, increased bearing capacity, tension membrane effect, and separation. These mechanisms have been extensively described in the references [8-11]. In parallel, tire pressure is a key factor in determining the magnitude and distribution of stresses applied to pavement systems.

http://doi.org/10.30684/etj.2025.164322.2009
Received 22 August 2025; Received in revised form 82 November 2025; Accepted 08 November 2025; Available online 27 November 2025
2412-0758/University of Technology-Iraq, Baghdad, Iraq

Increased tire pressures reduce the contact area, which in turn raises vertical contact stresses. These stresses accelerate fatigue and rutting, especially in the asphalt surface and subgrade layers [12]. Roberts et al. [13], noted that actual tire pressures in service often exceed those assumed in design, resulting in higher tensile strains and more rapid deterioration of thin flexible pavements. Marshek et al. [14], found that while axle load primarily influences rutting and subgrade strain, tire pressure significantly increases tensile strains and compressive stress within the asphalt layer. Over-inflated tires concentrate stresses under the tire's centerline, raising the risk of structural failure.

Moreover, experimental studies by Bonaquist et al. [15], showed that increasing contact tire pressure from 76 psi to 140 psi resulted in fatigue damage equivalent to adding 2,000 lbs of axle load . Sebaaly and Tabatabaee [16], reported that the most severe strain responses occurred in thin asphalt layers when wide-base radial tires were used .

Despite several studies on the effects of tire pressure and geosynthetic reinforcement, limited research has investigated their combined influence, particularly in scaled physical models of flexible pavements over weak subgrades. Understanding this interaction is crucial for optimizing pavement design under increasingly variable loading conditions. This study addresses this gap by evaluating the structural response of geotextile-reinforced flexible pavement models constructed over weak subgrades under various tire contact pressures.

This study aims to investigate the structural response of scaled models of flexible pavements reinforced with geotextiles, subjected to various tire pressures over weak subgrade conditions. The specific objective is to simulate different tire pressure levels (480, 560, 690) kPa, which represent low, moderate, and high pressure, and assess their influence on pavement performance metrics such as surface rutting, vertical stress at the bottom of the asphalt layer, and compressive vertical stress at the top of the subgrade.

2. Materials and test methods

2.1 Pavement materials

Test sections were composed of four layers: a compacted clay subgrade, a well-graded subbase, a stabilized base, and an HMA wearing surface. In reinforced sections, a polyester nonwoven geotextile was placed at two levels of the asphalt layer: the middle depth of the asphalt layer, and at the surface-base interface.

2.1.1 Subgrade soil

The subgrade soil was clay soil obtained from a construction site in Baghdad city. It is classified as an A-7 soil, according to the AASHTO classification, with a group index of 88.2. It is also classified as a lean clay soil with low plasticity (CL) according to the Unified Soil Classification System (USCS), characterized by a low Plasticity index of 23.36% and a liquid limit of 42.86%. The specific gravity (Gs) was found to be 2.690, and the optimum moisture content was 16.8%, as illustrated in Table 1. The CBR test (ASTM D1833-87) was used to characterize the subgrade soil index strength during the testing program. To place the lifts' subgrade soil at a low CBR, it was necessary to examine the unsaturated CBR at different water contents to choose the worst conditions that result in low CBR. To achieve this, a CBR (unsoaked) testing program was devised and conducted. It is essential to note that the moisture content was increased to a higher level to create weak subgrade soil; therefore, the soil was compacted at a level exceeding the optimum water content of 26% to achieve a CBR value of 2.1%, as shown in Figure 1.

2.1.2 Subbase material

The sub-base was obtained from the Al-Ubaidei asphalt plant, which is commonly used in the construction of flexible pavements. Routine laboratory tests were conducted on subbase materials to determine their properties, including sieve analysis, dry unit weight, and CBR ratio with compaction to 95% of the maximum dry density, according to the specifications of the State Organization of Roads and Bridges, Standard Specification for Roads and Bridges (SCRB, 2003). The compaction curve of the sub-base material is shown in Figure 2, and Table 1 lists the physical and mechanical properties of the sub-base material with the corresponding specifications. The standards show that the subbase material was type B, and Table 2 presents the gradation of the subbase material.

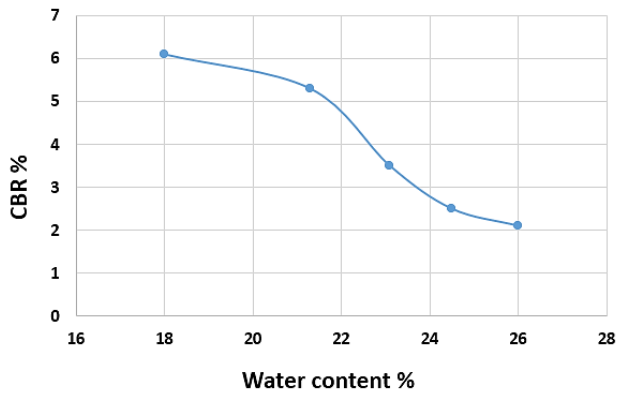

Figure 1: Differences in soil CBR according to moisture content

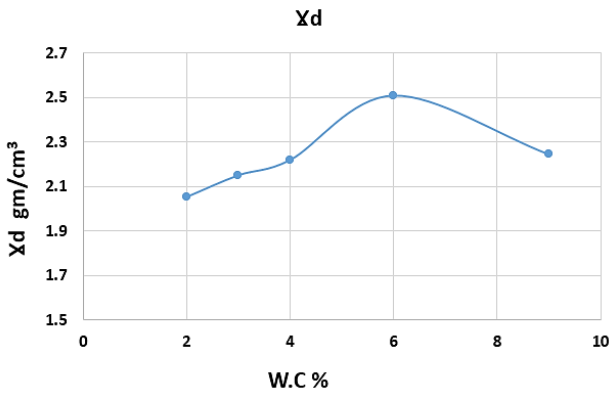

Figure 2: Subbase standard compaction curve

Table 1: Physical and mechanical test for subgrade and subbase material

Tests	Subgrade	Subbase	Specifications
Liquid Limit %	42.86	22	ASTM D 4318
Plastic Limit %	19.5	0	ASTM D 4318
Plasticity Index %	23.36	Na	ASTM D 4318
Specific gravity	2.690	2.57	ASTM D -854-14
Maximum dry Density g/cm^3	1.75	2.50	ASTM D 1557-07
Optimum Moisture Content %	16.8	6 %	ASTM D 2216
CBR @ 95 % Compaction	8.2	35.10 %	ASTM D 1883
Classification of Soil	CL	GW-GM	USCS
Cu		83.3	
Cc		1.01	

Table 2: Iraqi standards for wearing, base, and subbase coarse aggregate gradation (SCRB, 1983-R6)

Sieve Size "mm"	Sieve No. "inch"	Aggregate Material Gradation					
		Wearing Course		Base course		Subbase Course	
		Iraqi Standards Passing %	Blending %	Iraqi Standards Passing %	Blending %	Iraqi Standards Type B	Passing %
50.8	2	----	----	----	----	100	100
37.5	1.5			100	100	75-95	90.6
25	1			90-100	95	----	----
19	¾			76-90	83	----	----
12.5	½	100	100	56-80	68	----	----
9.5	3/8	80-100	88	48-74	61	40-75	57.5
4.75	No. 4	46-76	60	29-59	44	30-60	41.5
2.36	No. 8	28-58	41	19-45	32	21-47	30.5
0.3	No. 50	8-24	17	(5-17)	11	14-28	17.2
0.075	No. 200	4-12	9	(2-8)	5	5-15	2.3

2.1.3 Asphalt binder

The asphalt binder used to prepare the asphalt concrete mixture for the wearing surface course and bituminous base was a (40-50) penetration grade supplied from Al-Dura Refinery. Table 3 presents the physical properties of the asphalt binder used in this study.

Table 3: Asphalt binder properties

Test	ASTM designation	Test results	SCRB specification
Penetration (25 ℃ 100 g .5 sec)	D5	45	40-50
Ductility (35 ℃. 5 cm/min)	D113	113	>100
Softening Point,	D36	55	---
Flash Point, °C	D92	294	>232
Fire Point, °C	D92	307	---
Specific Gravity of Asphalt	D72	1.035	---
Rotational Viscometer (Pa. sec)	D4402	0.481@ 135	---
		0.122 @165	---
Loss on Heating (5hrs at 163 ℃)	D1754	0.27%	<0.75
Absolute viscosity at 60 ℃, poises		2033	
Solubility in trichloroethylene		99.73%	≥ 99

2.1.4 Base course material

The aggregates for the base material were supplied from Al-Ubaidei Asphalt Plant. The gradation of base course material is presented in Table 2. A stabilized course with (40-50) grade asphalt, designed according to the Marshall design procedure, with an optimum asphalt content of 3.7%, air voids of 4.1%, and density of 2.311 kg/cm3, as shown in Table 4.

2.1.5 Asphalt concrete layer

The HMA wearing surface met the Iraqi specifications for wearing courses, using a nominal aggregate size of 19 mm. The asphalt content used was 4.8 %. Typical HMA mix properties included 10.10 kN stability, a maximum specific gravity of 2.57, voids in total mix of 4.1%, and voids in mineral aggregate (VMA) of 15.5% as illustrated in Table 4.

Table 4: Bituminous base course and wearing course mix properties

Properties	Base		Wearing course	
	Result	Specification	Result	Specification
Asphalt Percent (40-50) Penetration	3.7 %	3.0 - 5.5	4.8	4.0-6.0
Stability kN	9.4	Min. 5	10.10	Min. 8
Flow mm	3.1	2 – 4	3.3	2 – 4
VTM %	4.1	3 – 6	4.1	3 – 5
VMA%	14.4	-----	15.5	-----
VFB %	71.5	-----	73.5	70-85
Density (g/cm^3)	2.311	-----	2.307	-----
Deleterious Material %	1.29	Max. 3 %	1.314	Max. 3 %
Soundness $MgSO_4$ %	0.0705	Max. 18 %	0.121	Max. 18 %

3. Geosynthetic materials

The geotextile used in this study was a polyester (PET) staple fiber, needle-punched nonwoven geotextile (PET NW130), supplied by Shandong XiuHe Engineering Materials Co., Ltd., a well-known company specializing in engineering materials in China. The geotextile was installed at two locations within the pavement model: Interface between the asphalt layer and the stabilized base, and mid-depth of the asphalt layer.

Figure 3 shows the geotextile used, and its technical specifications are listed in Table 5 as provided by the manufacturer company. The material was selected for its balance of tensile strength, filtration capacity, and durability, making it suitable for reinforcement and separation in flexible pavement systems.

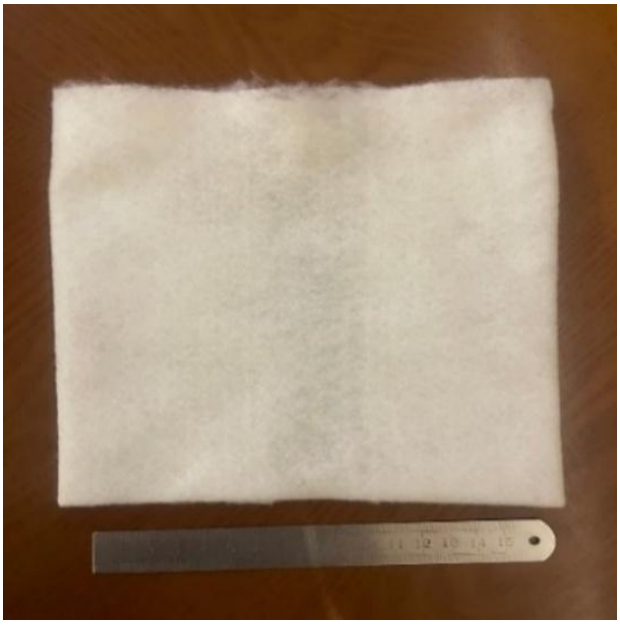

Figure 3: Nonwoven geotextile (PET NW130)

Table 5: Specifications of pet nonwoven geotextile (PET NW130)

Properties	Test Method	Unit	PET NW130
Tensile Strength (MD/TD)	ASTM D4595	kN/m	4
Tensile Elongation (MD/TD)	ASTM D4595	%	50
Grab Tensile Strength (MD/TD)	ASTM D4632	N	200
Trapezoidal Tear Strength (MD/TD)	ASTM D4533	N	100
CBR Burst Strength	ASTM D6241	N	400
Pore Size O95	ASTM D4751	µm	200
Water Flow Q100	ASTM D4491	L/m^2/s	300
U.V. Resistance	ASTM D4355	%@500h	70
Thickness	ASTM D5199	mm	1.1
Weight	ASTM D5261	g/m^2	130
Roll Width	-	m	2
Roll Length	-	m	50

4. Pavement model design

4.1 Experimental setup and scaled models

In this study, a 1/3 physical scale model was employed to simulate the structural response of a flexible pavement under repeated axle loading. The prototype full-scale pavement was selected in accordance with the structural design for Iraqi Expressway No. 1, which consists of a 4 cm wearing surface, an 8 cm binder course, a 20 cm bituminous base, a 25 cm compacted subbase, and a 150 cm subgrade thickness. The corresponding scaled model comprised layers of 5.0 cm asphalt, 6.0 cm bituminous base, 9.0 cm subbase, and 50.0 cm subgrade, resulting in a total thickness of 70 cm.

A pneumatic tire with an external diameter of 30.5 cm was used in the model to represent a single axle load with a dual tire. Based on a 1/3 scale, the prototype with a half single standard axle load with dual tire of 40 kN was scaled down to an equivalent model load of approximately 5.0 kN to maintain stress similarity between the model and full-scale system. The repeated load was applied using a 3.0 kW hydraulic actuator, with loading frequencies of 0.21 Hz, appropriate for pavement response studies because higher wheel speeds lead to reduced maximum compressive and tensile strains, as the asphalt mixture becomes stiffer at higher frequencies [17-18]. The load of 5 KN (480 kPa) was adjusted to achieve different pressures, allowing for the study of additional scenarios representing moderate and high pressures. The additional loads were 6.5 kN and 7.5 kN, corresponding to pressures of 560 kPa and 690 kPa, respectively.

4.2 Tire pressure simulation setup

Tire pressure was simulated using a mechanical load frame through an accelerated load test assembly equipped with pneumatic actuators and a rigid tire moving in a unidirectional path, which applied varying contact pressures depending on the applied load, ranging from 400 kPa to 800 kPa, representing typical commercial vehicle pressures, as shown in Figure 4. The actual tire–pavement contact area under the scaled load was determined experimentally using the color spray method. The load contact area was calculated as an equivalent area of a rectangle with dimensions (8.5×12.3) cm, (8.9×13) cm, and (8.7×12.6) cm for 480, 560, and 690 kPa pressure, respectively, to simulate real tire-pavement interaction [19]. The loading setup was designed to enable repeated loading at controlled pressures, simulating the stress cycles induced by traffic.

Figure 4: Loading set up

4.3 Construction of the scaled model of flexible pavement

The scaled pavement models were constructed layer by layer within a rigid steel test box with dimensions of 2.0 m in length, 1.0 m in width, and 0.70 m in depth. Before placement, the joints of the metal box were sealed with silicone, and a layer of nylon sheet was placed inside the container to prevent loss of targeted moisture content, as shown in Figure 5(a). Each material layer was carefully prepared and compacted to achieve the target density and moisture content, as determined by the laboratory compaction results, as illustrated in Figure 5(b-c-d-e). The subgrade soil was compacted in multiple lifts to achieve the target CBR of 2.1%, simulating weak subgrade conditions. The first lift was 10 cm thickness compacted manually using hand tamper, as shown in Figure 5 (b), the second and third lifts were 20 cm thickness compacted using a Robin Plate compactor EY20 with a net weight 100 kgs and 5.0 Hp engine, which is suitable for asphalt, soil, sand, gravel, and mixer soils in the areas of civil, or road engineering as presented in Figure 5(g). A 3 cm thick cork layer was placed at the box sides and beneath the subgrade to minimize stress wave reflections from the rigid box bottom and provide a more realistic boundary condition. The subbase, bituminous base layers, and asphalt wearing surface were constructed and compacted to the target density in one lift with thicknesses of 9.0 , 6.0 , and 5.0 cm, respectively, using the same plate compactor as illustrated in Figure 5(f-g). For reinforced sections, a polyester nonwoven geotextile was installed at the surface-base interface and at the middle depth of the surface layer during construction, shown in Figure 5(h-i). Table 6 shows the test pavement sections, while Figure 6 presents the pavement section structure.

Table 6: Pavement test sections

Section	Type of Geosynthetics	Location of Geosynthetics
Section 1	Non	Control
Section 2	Nonwoven geotextile	Surface - Base Interface
Section 3	Nonwoven geotextile	Middle of Surface Thickness

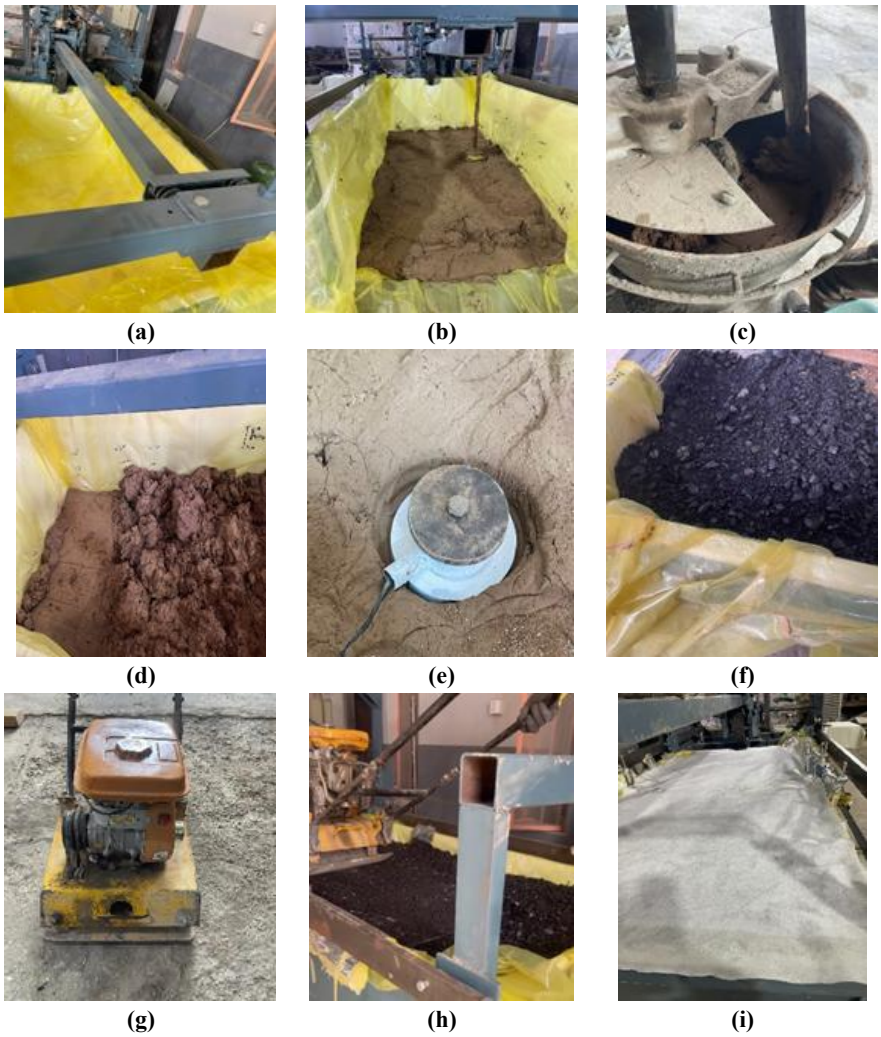

Figure 5: (a-i) Scaled model of the flexible pavement construction

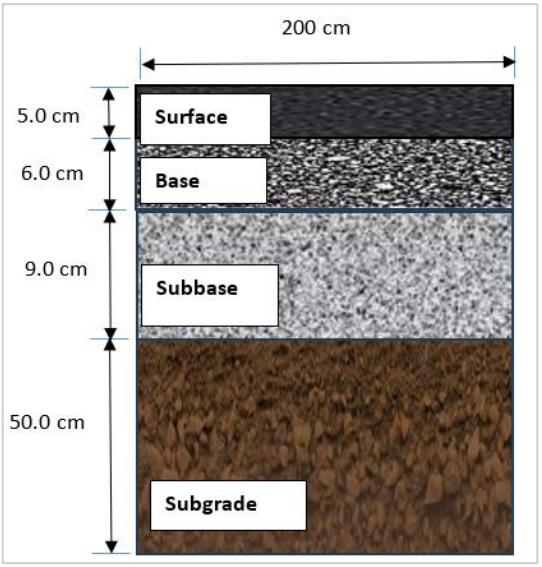

Figure 6: Pavement test section structure

4.4 Data collection methods (e.g., load cells, displacement sensors)

To measure the response of the pavement under repeated wheel loading, a system of load pressure cell sensors has been set up. For vertical load applied at the top of the subgrade and at the bottom of the asphalt surface layer, high-precision load pressure cells are installed. The device accommodates approximately 750 load cycle applications per hour, corresponding to a speed of 4.75 km/h (1.320 m/s) and a frequency of 0.21 Hz. Real-time load, stress, and surface rutting data were recorded every 750 cycles, corresponding to approximately every hour, and synchronized with the loading actuator using the data collection system during each test sequence.

5. Results and discussion

The scaled test sections are prepared to evaluate the performance of a flexible pavement resting on a weak subgrade under varying tire pressures, with and without geotextile reinforcement. All sections were subjected to identical loading conditions (5, 6.5, and 7.5) KN and tire pressure of (480, 560, and 690) kPa, which represent low, moderate, and high tire pressure, respectively. The performance indicators measured were the vertical stress at the bottom of the asphalt surface and the vertical stress at the top of the subgrade layer, both for 25,000 load cycles.

5.1 Vertical stress at the bottom of the asphalt layer

Figure 7(a-c) presents the vertical stress at the bottom of the asphalt surface layer for different tire pressures (480, 560, and 690) kPa for three pavement test sections, one control, and the two other reinforced sections. The vertical stress increases with the increase in tire pressure and loading cycles. In the first 5,000 cycles, stress gradually increases, possibly due to compaction and densification of the surface and base course, and then remains in a relatively steady state. Table 7 illustrates the variation in the percentage increase in stress value under different pressures. The increase in contact tire pressure increases vertical stress at the bottom of the asphalt surface layer among all test sections. Section 3, which is reinforced at the mid-depth of the asphalt wearing surface, exhibits the highest percentage (74.4%) of stress, ranging from the lowest to the highest contact tire pressure, compared to Section 1 (70.9%) and Section 2 (71.4%). This could be attributed to the reduction in layer thickness above the geotextile, which cannot dissipate the load effects. This trend aligns well with [2,12-14].

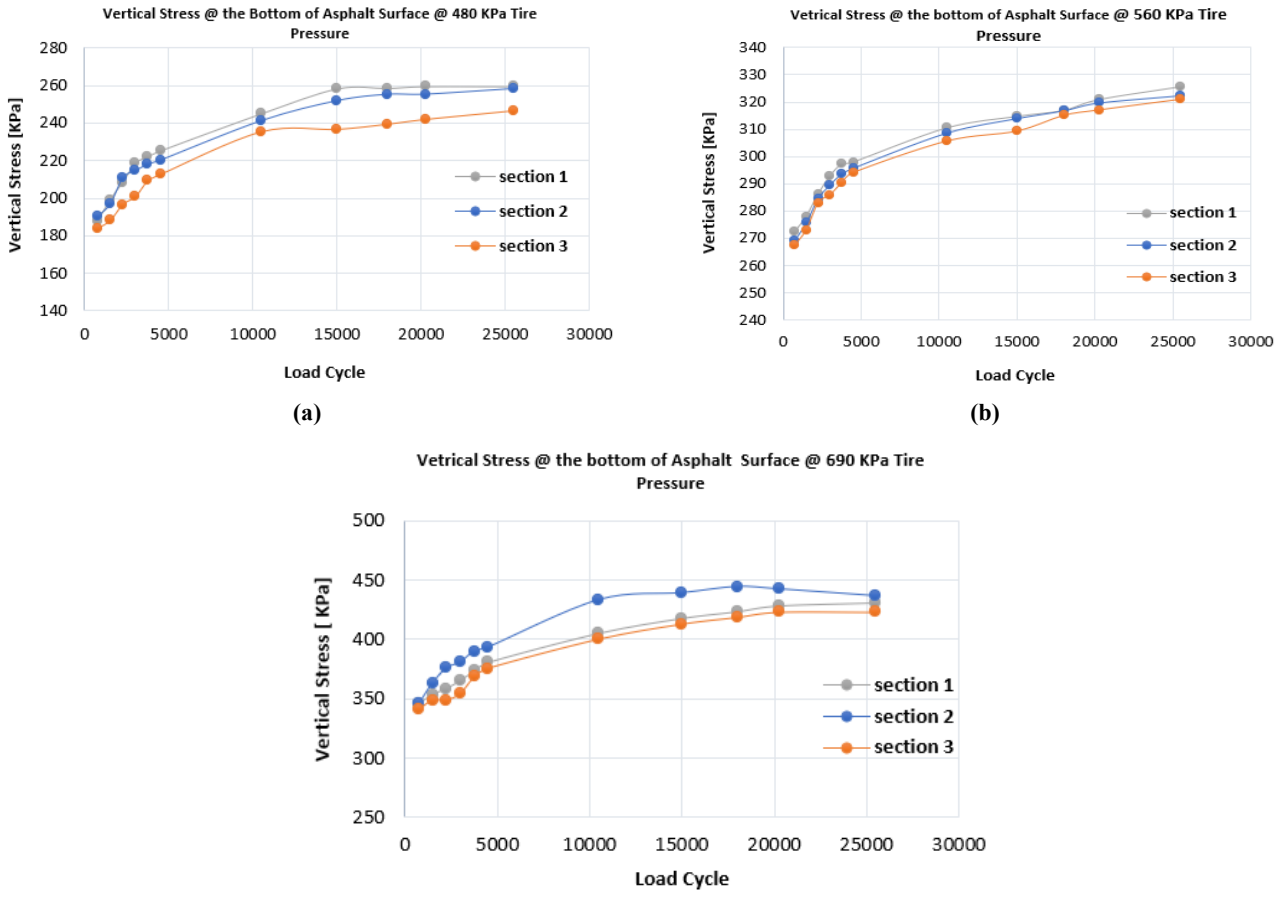

Figure 7: Vertical stress at the bottom of asphalt surface layer a) 480 kpa tire pressure, b) 560 kpa tire pressure, c) 690 kpa tire pressure

Table 7: Maximum vertical stress at the bottom of asphalt layer

Sections	Tire Pressure Kpa				
	480	560	690	% Increase from the lowest pressure	% Increase from the moderate pressure
Section 1	259.66	325.81	443.76	70.9	36.2
Section 2	259.47	322.314	444.727	71.4	38.0
Section 3	246.32	320.99	429.5	74.4	33.8

5.2 Vertical stress at the top of subgrade

Vertical stress at the top of the subgrade was measured directly under the wheel path at different tire pressures (480, 560, and 690 kPa), as illustrated in Figure 8 (a-c). Similarly, all sections exhibit increasing stress values as tire contact pressure increases. Additionally, the vertical stress increases gradually at the first 5,000 load cycles, then increases at a steady rate, as shown in Figure 8. The maximum percent stress increase observed at the 690 kPa level of pressure was approximately 58.9%, 73.7%, and 83.6% for sections 1, 2, and 3, respectively, from the lowest tire pressure of 480 kPa to the highest pressure of 690 kPa. These observations indicate that section 3 has the highest sensitivity to tire pressure increase. In contrast, the increases were approximately consistent at 33.8%, 33.5%, and 33.7% from the moderate tire pressure of 560 kPa, as illustrated in Table 8. This could be attributed to a reduction in the membrane effect of the geotextile under high pressure, resulting from the shallow depth, which leads to a high concentration of stress at the top of the subgrade, as reported by Chatrabhuj, K Meshram [20].

Table 8: Maximum vertical stress at the top of subgrade layer

Sections	Tire Pressure Kpa				
	480	560	690	(%) Increases from the lowest pressure	% Increases from the moderate pressure
Section 1	28.42	33.75	45.144	58.9	33.8
Section 2	25.637	33.349	44.537	73.7	33.5
Section 3	24.255	32.802	44.52	83.6	35.7

The steep increase in vertical stresses recorded at 690 kPa contact pressure confirms that higher contact pressure can significantly accelerate pavement deterioration, which is consistent with [12-16] who all reported increases in vertical stress with elevated tire pressure.

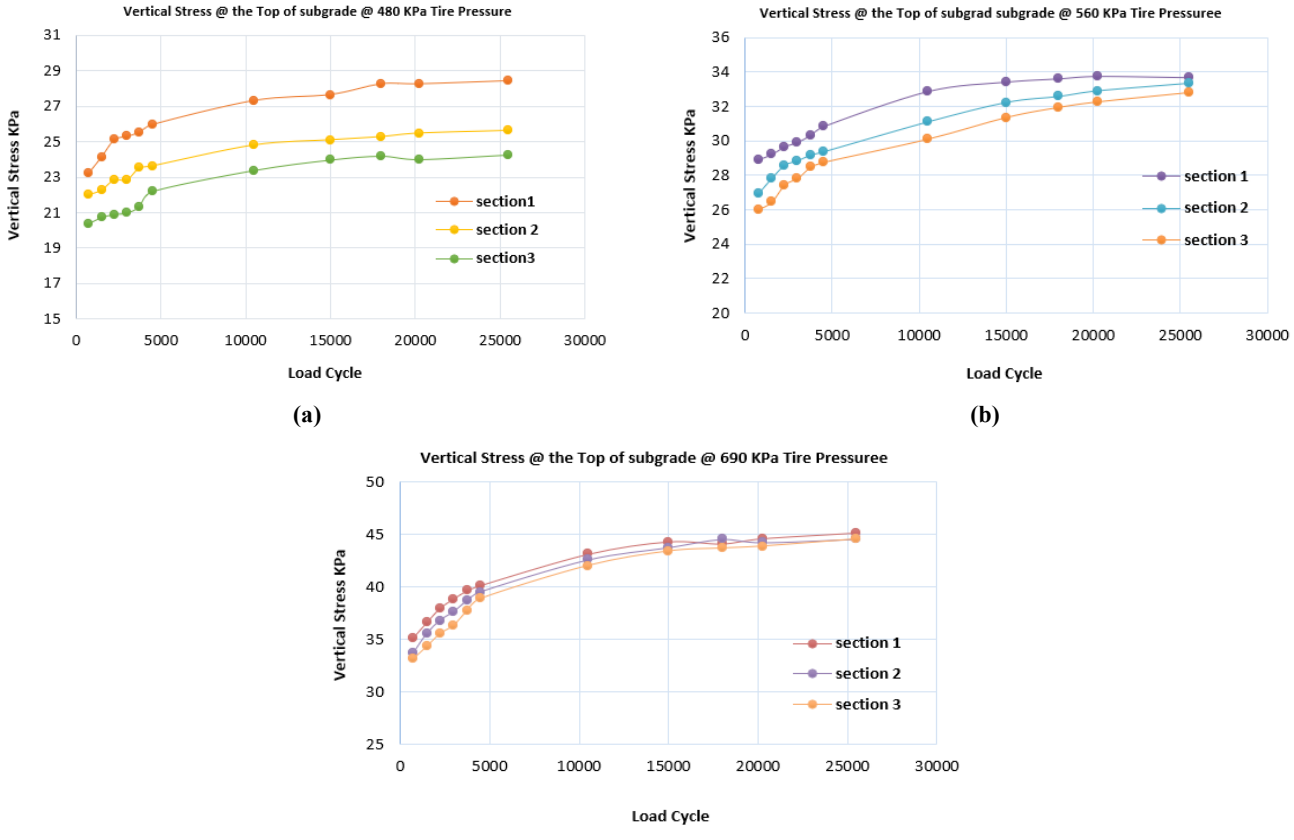

Figure 8: Vertical stress at the top of subgrade layer a) 480 kpa tire pressure, b) 560 kpa tire pressure, c) 690 kpa tire pressure

5.3 Effect of geotextile reinforcement

Figure 9 illustrates the mean vertical stress at the bottom of the asphalt layer that rose uniformly with the applied contact pressure in each case for all sections. The evaluated stresses measured at 480 kPa exhibited a slight variation across the three sections (244.099, 241.348, and 228.225 kPa) for control sections 1, 2, and 3, respectively, indicating consistent performance under reduced loading. All sections with increasing pressure also showed higher stress values, as seen at 560 kPa and 690 kPa. However, at a pressure of 560 kPa, the stress remained approximately the same (309.777, 307.997, and 304.82) kPa for the control sections 1, 2, and 3, respectively. The additional contact pressure made even worse the stress value, reaching changing rates more pronounced at a higher-pressure level of 690KPa, showing (407.438, 424.211, and 401.622) kPa for the three sections, respectively. Section 2 had the highest levels of stress at 690 kPa, followed by Section 1, and then so on for the other ranges (Section 3 is always a little less than the two other sections). While this trend suggests that geotextile reinforcement materials are effective at distributing loads at low tire pressure levels, differences in reinforcement location can affect the stress response to some extent, possibly resulting in slightly larger stress reductions for Section 3 under the test conditions.

Figure 10 illustrates the variation in average vertical stress at the top of the subgrade for contact pressures of 480, 560, and 690 kPa in geotextile-reinforced sections, compared to the control section without reinforcement. The stress was higher in the control section 1 at the lowest range of contact pressure (27.179 kPa), and it was decreased moderately at section 2 to (24.640 kPa), then remained approximately the same at higher contact pressure (23.296 kPa), which demonstrated a clear stress reduction due to geotextile reinforcement. When the contact pressure increased to 560 kPa, the differences among sections diminished; however, Section 3 still showed less stress relative to the control, Section 1. At the highest contact pressure (690 kPa), all sections exhibited high stress values exceeding 40 kPa, with little variation, indicating that stress reduction is diminished under higher applied loads. This is attributed to the fact that the placement of geotextile reinforcement under or within the wearing surface could minimize the tension membrane effect due to shallow depth, so that the effect could be reduced or lost under high pressure, and the geotextile cannot intercept the critical shear zones that develop deeper in the pavement, leading to concentrated stress at the top of the subgrade. In general, Section 3 exhibited better performance in stress attenuation. Under lower contact pressures, the reinforcement of the geotextile was more effective in reducing subgrade stress. These results are consistent with the established literature [12-16] indicated higher stress level with higher tire pressure, while [8],[2], and [4-9], all documented the effectiveness of geosynthetics in minimizing deformations and improving load distribution of pavement built over weak subgrade.

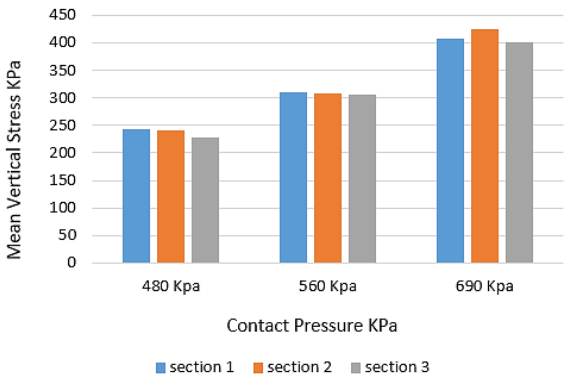

Figure 9: Comparison between mean vertical stress at the bottom of asphalt surface

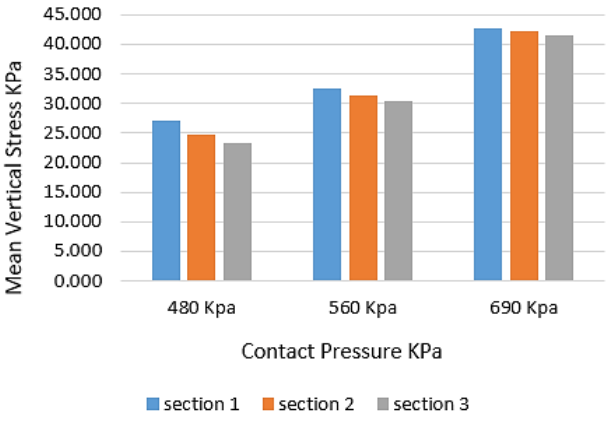

Figure 10: Comparison between mean vertical stress at the top of subgrade

6. Conclusion

Using scaled models of flexible pavements reinforced with geotextiles, this study examines the structural response to a range of tire pressures under weak subgrade conditions. The following are the key conclusions based on the conducted experimental work for the current research:

1) Tire contact pressure strongly affects the stress responses of flexible pavements, with higher pressures (690 kPa) producing up to 74.4 % higher stresses at the bottom of the asphalt layer and up to 83.6 % higher stresses at the top of the subgrade compared to the lowest pressure (480 kPa).
2) Geotextile reinforcement reduced stress levels transmitted to the subgrade, especially at lower tire pressures, where reductions were most pronounced.
3) Reinforcement placement at the middle depth of the asphalt surface layer provided slightly better performance than placement at the base–surface interface in terms of stress reduction.

4) At high contact tire pressures, the advantage of geotextile reinforcement was significantly diminished, indicating that excessive pressure can diminish reinforcement benefits.

Author contributions

Conceptualization, **N. Salman**, and **H. Joni**; data curation, **N. Salman**; formal analysis, **N. Salman**; investigation, **N. Salman**; methodology, **H. Joni** and **N. Salman**.; project administration, **H. Joni**; resources, **N. Salman**; software, **N. Salman**.; supervision, **H. Joni**; validation, **H. Joni** and **N. Salman**; visualization, **H. Joni**, and **N. Salman**; writing—original draft preparation, **N. Salman**; writing—review and editing, **N. Salman**. All authors have read and agreed to the published version of the manuscript.

Funding

This research received no specific grant from any funding agency in the public, commercial, or not-for-profit sectors.

Data availability statement

The data that support the findings of this study are available on request from the corresponding author.

Conflicts of interest

The authors declare that there is no conflict of interest.

References

[1] S. Tasnim, F. U. A. Shaikh, P. Sarker, S. I. Doh, J. A. A. Albtoosh, A comprehensive review of flexible pavement failures, improvement methods, and their disadvantages, Key Eng. Mater., 879 (2021) 136–148. https://doi.org/10.4028/www.scientific.net/KEM.879.136

[2] A. F. Jasim, M. Y. Fattah, I. F. Al-Saadi, A. S. Abbas, Geogrid reinforcement optimal location under different tire contact stress assumptions, Int. J. Pavement Res. Technol., 14 (2021) 357–365. https://doi.org/10.1007/s42947-020-0145-6

[3] I. L. Al-Qadi, P. J. Yoo, M. A. Elseifi, I. Janajreh, G. Chehab, A. Collop , Effects of tire configurations on pavement damage, J. Assoc. Asphalt Paving Technol., 74 (2005) 921–961. https://trid.trb.org/View/777867

[4] G. Jayalath, C. Prasad, C. Gallage, M. Dhanasekar, B. Dareeju, J. Ramanujam, J. Lee, Pavement model tests to investigate the effects of geogrid as subgrade reinforcement, in: 12th Aust. & N. Z. Young Geotechnical Professionals Conf., Australian Geomechanics Soc., 2018, 1–8.

[5] Nazzal, M. D. Laboratory characterization and numerical modeling of geogrid reinforced bases in flexible pavements. Ph.D. Thesis, Louisiana State University, Baton Rouge, LA, 2007. https://doi.org/10.31390/gradschool_dissertations.3889

[6] M. Abu-Farsakh, M. Nazzal, Evaluation of the base/subgrade soil under repeated loading: Phase I – laboratory testing and numerical modeling of geogrid reinforced bases in flexible pavement, Report No. FHWA/LA.09/450, Louisiana Transportation Research Center, 2009.

[7] S. F. Ibrahim, N. G. Ahmed, D. E. Mohammed, Effect of reinforcement on improved surface pavement for weak subgrade conditions, Int. J. Geomate., 11 (2016) 2188–2193.

[8] J. G. Zornberg, Advances in the use of geosynthetics in pavement projects, in: Proc. 2nd Iberic Conf. on Geosynthetics, Geosintec Iberia, 2015.

[9] E. V. Cuelho, S. W. Perkins, Geosynthetic subgrade stabilization – field testing and design method calibration, Transp. Geotech., 10 (2017) 22–34. https://doi.org/10.1016/j.trgeo.2016.10.002

[10] H. Alimohammadi, V. R. Schaefer, J. Zheng, H. Li, Performance evaluation of geosynthetic reinforced flexible pavement: a review of full-scale field studies, Int. J. Pavement Res. Technol., 14 (2021) 30–42. https://doi.org/10.1007/s42947-020-0019-y

[11] C. Jayalath, C. Gallage, K. Wimalasena, J. Lee, J. Ramanujam, Performance of composite geogrid reinforced unpaved pavements under cyclic loading, Constr. Build. Mater., 304 (2021) 124570. https://doi.org/10.1016/j.conbuildmat.2021.124570

[12] I. L. Al-Qadi, H. Wang, Prediction of tire-pavement contact stresses and analysis of asphalt pavement responses: A decoupled approach, Asphalt Paving Technol. – Proc. Assoc. Asphalt Paving Technol., 80 (2011) 289.

[13] F. L. Roberts, J. Tielking, D. Middleton, R. L. Lytton, K. Tseng, Effects of tire pressures on flexible pavements. Final report, Report No. FHWA/TX-86/372-1F, 1985.

[14] K. M. Marshek, H. H. Chen, R. B. Connell, C. L. Saraf, Effect of truck tire inflation pressure and axle load on flexible and rigid pavement performance, Transp. Res. Rec., 1070 (1986) 14–21.

[15] Bonaquist, R. , Churilla, C. , Freund, D. Effect of load, tire pressure, and tire type on flexible pavement response; Public Roads, 1988.

[16] P. Sebaaly, N. Tabatabaee, Effect of tire pressure and type on response of flexible pavement, Transp. Res. Rec., 1227 (1989) 115-127.

[17] Jing, R. A. Varveri, X. Liu, A. Scarpas, S. Erkens. 2020. Study on the asphalt pavement response in the accelerated pavement testing facility, in: Proc. 9th Int. Conf. on Maintenance & Rehabilitation of Pavements (Mairepav9), Springer, Cham, Vol. 76, pp. 871–880. https://doi.org/10.1007/978-3-030-48679-2_81

[18] N. Garg, G. F. Hayhoe, Asphalt concrete strain responses at high loads and low speeds at the national airport pavement test facility (NAPTF), in: Advancing Airfield Pavements, 2001, pp. 1–14. https://doi.org/10.1061/40579(271)1

[19] Huang, Y. H. Pavement analysis and design, Vol. 2, Pearson/Prentice Hall, Upper Saddle River, NJ, 2004.

[20] C. Chatrabhuj, K. Meshram, Use of geosynthetic materials as soil reinforcement: an alternative eco-friendly construction material, Discov. Civ. Eng., 1 (2024) 41. https://doi.org/10.1007/s44290-024-00050-6